Precision model-independent bounds from a global analysis of $b \to c\ell\nu$ form factors

Thomas D. Cohen,[1,*] Henry Lamm ⬤,[1,†] and Richard F. Lebed[2,‡]

[1]*Department of Physics, University of Maryland, College Park, Maryland 20742, USA*
[2]*Department of Physics, Arizona State University, Tempe, Arizona 85287, USA*

We present a model-independent global analysis of hadronic form factors for the semileptonic decays $b \to c\ell\nu$ that exploits lattice-QCD data, dispersion relations, and heavy-quark symmetries. The analysis yields predictions for the relevant form factors, within quantifiable bounds. These form factors are used to compute the semileptonic ratios $R(H_c)$ and various decay-product polarizations. In particular, we find $R(D_s^*) = 0.20(3)$ and $R(J/\psi) = 0.25(3)$, predictions that can be compared to results of upcoming LHCb measurements. In developing this treatment, we obtain leading-order nonrelativistic QCD results for the nonzero-recoil relations between the $B_c^+ \to \{J/\psi, \eta_c\}$ form factors.

I. INTRODUCTION

While the Higgs interaction is the only source of *lepton universality* violations within the Standard Model (SM), the observation of neutrino masses implies that at least one form of beyond-SM modification exists, specifically in the lepton sector. The factorization of QCD dynamics from electroweak interactions in the SM allows amplitudes for semileptonic decays to be expressed as the familiar product of hadron ($H^{\mu\nu}$) and lepton ($L^{\mu\nu}$) tensors at leading order:

$$|\mathcal{M}_{\bar{b} \to \bar{c}\ell^+\nu_\ell}|^2 = \frac{L_{\mu\nu}H^{\mu\nu}}{q^2 - M_W^2} + \mathcal{O}(\alpha, G_F). \quad (1)$$

Heavy-hadron semileptonic decay rates (both full and differential) producing distinct lepton flavors differ only due to factors of lepton mass that arise from kinematic and helicity-flip factors. Such dependences can be removed in a variety of ways [1–9]. Measurements from *BABAR*, Belle, and LHCb of the ratios $R(D^{(*)})$ [10–19] of the heavy-light meson decays $B \to D^{(*)}\ell\nu$, with $\ell = \tau$ to $\ell = \mu$, exhibit a combined 3.1σ discrepancy with the HFLAV-suggested SM values [20], which averages the results of Refs. [6, 21–23]. Recently, the LHCb Collaboration has measured $R(J/\psi)$ [24], which is within 1.3σ [25] of the SM prediction.

*cohen@umd.edu
†hlamm@umd.edu
‡Richard.Lebed@asu.edu

These results, including lattice-determined and theoretically computed values of $R(H_c)$, are compiled in Table I.

In the future, it would be useful to consider other semileptonic decays. Run III of LHCb may open the opportunity to measure $R(D_s^{(*)})$ [34]. A determination of $R(\eta_c)$ would be exciting. However, $R(\eta_c)$ is substantially harder to measure than $R(J/\psi)$ for a few reasons, the foremost of which is the absence of a clean η_c decay process with a substantial branching fraction (analogous to $J/\psi \to \mu^+\mu^-$) for reconstructing the η_c; this leads to large backgrounds. Additionally, the transition from excited charmonium states to η_c is poorly understood, which further complicates the extraction of signals [35].

In order to fully leverage all of these experimental results, it is necessary to have rigorous predictions from the SM for all of these ratios. Even setting aside the very interesting issue of lepton universality, determining hadronic form factors is important in its own right, as each such function represents a wealth of information about nonperturbative QCD. Form factors are not completely unconstrained, however. They must satisfy well-known model-independent constraints that follow from bedrock

TABLE I. Existing results for $R(H_c)$ from experiment, predictions from lattice QCD alone, and theoretical values including additional inputs.

H_c	R_{exp}	R_{lat}	R_{theory}
D	0.340(27)(13) [10–13]	0.300(8) [26–28]	0.299(3) [20]
D^*	0.295(11)(8) [10–19]	⋯	0.258(5) [20]
D_s	⋯	0.2987(46) [29]	⋯
Λ_c	⋯	0.3328(74)(70) [30]	0.324(4)[31]
J/ψ	0.71(17)(18) [24]	[0.20,0.39] [25]	⋯
η_c	⋯	0.30(4) [32,33]	⋯

principles of quantum field theory, specifically unitarity and the complex analyticity of their Green's functions as functions of momentum variables at all values, except when a resonance, particle-creation threshold or other special kinematic configuration is realized. In the case of semileptonic decays, the form factors can be parametrized as a product of known functions representing resonant poles and other nonanalytic structures in the corresponding Green's function, times a Taylor series in a conformal variable that tracks the momentum transfer; the Taylor coefficients are constrained in magnitude by unitarity. This is the *Boyd, Grinstein, and Lebed (BGL)* parametrization [36,37] (see Ref. [38] for a brief review of its historical antecedents).

The constraint of unitarity in model-independent approaches such as the BGL parametrization has historically been underutilized because fits to experiment typically consider only a single exclusive process (e.g., $B \to D^* \ell \nu$). However, each exclusive channel appearing in the two-point Green's function for $b \to c$ currents positively contributes to the unitarity bound, and therefore a simultaneous fit including multiple processes provides stronger constraints on each of the individual processes [6,23,37].

The purpose of this work is to perform a global analysis within the BGL parametrization of lattice-QCD data for seven exclusive hadronic $b \to c$ processes: $B \to \{D, D^*\}$, $B_s \to \{D_s, D_s^*\}$, $B_c \to \{J/\psi, \eta_c\}$, and $\Lambda_b \to \Lambda_c$. We obtain the corresponding transition form factors. These form factors are computed directly from the SM and obtained within quantifiable bounds. Thus, they can be used to make reliable predictions from the SM that can directly confront experiment. We use them to compute three types of observables: the semileptonic decay ratios $R(H_c)$, the τ polarization $P_\tau(H_c)$, and the vector-meson longitudinal polarization fraction $F_L^{H_c}$.

The analysis presented here is essentially model independent. We do not use *ad hoc* model assumptions about the physical mechanisms dominating the form factor, beyond accepting the SM to identify allowed functional forms of the form factors. Rather, we use as input *ab initio* Monte Carlo calculations of QCD from the lattice as our principal input. Such data are quite limited; not all of the relevant form factors have been computed, and those that have are computed at a limited number of momentum-transfer values. The BGL parametrization using the unitarity bound allows us to extend our knowledge of the form factors to other momentum transfers, and to do so in such a way that the errors can be quantified. We can gain information about form factors that have not been directly computed on the lattice from those that have by exploiting emergent symmetries of QCD that become valid as the quark masses become large.

There are, of course, errors associated with truncating the series in BGL parametrization and truncating the expansion in the inverse heavy-quark mass. Fortunately, one has *a priori* estimates of their size, which allows for reliable SM predictions without invoking additional model dependence. However, some judgment is required in estimating their sizes quantitatively. We have therefore made very

conservative estimates in order to ensure that our predicted bounds are reliable enough so that the experimental measurements provide meaningful tests of the SM.

The lattice data that provide the input for the analysis has both statistical and systematic errors. The statistical errors can be easily incorporated into our bounds. In some cases, the major systematic errors have been well explored and estimated reliably and can also be incorporated in a straightforward way. However, in some cases, the only available lattice calculations do not provide estimates for some of the major systematic errors. In these cases, we add a systematic error in by hand, and do so in a very conservative manner, by assuming larger-than-realistic errors.

Thus, while the analysis is model independent, it does involve some *ad hoc* judgment in the assignment of systematic errors. As this was done quite conservatively, the principal effect is to make the error bounds for our final results larger than they otherwise would be. These effects can, of course, be mitigated by the constant improvement in the treatment of errors in lattice simulations.

We begin in Sec. II with a discussion of the $V - A$ weak-interaction structure of the SM responsible for semileptonic decays and the form factors under investigation. In Sec. III, we explain how heavy-quark symmetries can be used to obtain relations between the form factors of heavy-light systems and heavy-heavy meson systems. The lattice results used in this work are discussed in Sec. IV. Section V presents the dispersive-analysis framework utilized to constrain the form factors as functions of momentum transfer. The results of our analysis are presented in Sec. VI, and we conclude in Sec. VII.

II. STRUCTURE OF $\langle H_c | (V - A)^\mu | H_b \rangle$

Since the first-principles calculation of the leptonic tensor $L^{\mu\nu}$ in Eq. (1) is straightforward in the SM, the computation of semileptonic decay rates reduces to parametrizing exclusive components $\langle H_c | (V - A)^\mu | H_b \rangle$ of the hadronic tensor in terms of transition form factors. The tensor structure is expressed in terms of the hadron momenta, P^μ for H_b (with mass $M \equiv M_{H_b}$) and p^μ for H_c (with mass $m \equiv M_{H_c}$), and additionally the polarization ϵ^μ of the H_c if it is a vector meson, or heavy-quark spinors $u_{b,c}$ if $H_{b,c}$ are baryons. The only functional dependence of the form factors arises through the squared momentum transfer to the leptons, $t = q^2 \equiv (P - p)^2$. The various cases of phenomenological interest are now outlined.

A. $B \to D$, $B_s \to D_s$, $B_c^+ \to \eta_c$

If both $H_{b,c}$ are pseudoscalar mesons, then only two independent Lorentz structures, and hence two independent form factors, are possible:

$$\langle H_c(p) | (V - A)^\mu | H_b(P) \rangle$$
$$= f_+(t)(P + p)^\mu + f_-(t)(P - p)^\mu. \quad (2)$$

Indeed, the parity invariance of strong interactions precludes the current A^μ from providing a nonzero contribution to Eq. (2). In this work, we exchange $f_-(t)$ for the combination

$$f_0(t) \equiv (M^2 - m^2)f_+(t) + tf_-(t). \tag{3}$$

With this definition, one sees that $(M^2 - m^2)f_+(0) = f_0(0)$, a constraint upon two otherwise independent form factors that we will impose when fitting the functions. This normalization of f_0 differs by a mass-dependent prefactor from that used in lattice-QCD calculations [26–29,39]:

$$f_0(t) = (M^2 - m^2)f_0^{\text{lat}}(t). \tag{4}$$

The differential decay rate for this semileptonic decay process is

$$\frac{d\Gamma}{dt} = \frac{G_F^2 |V_{cb}|^2}{192\pi^3 M^3} \frac{k}{t^{5/2}} (t - m_\ell^2)^2 [4k^2 t(2t + m_\ell^2)|f_+|^2 \\ + 3m_\ell^2 |f_0|^2], \tag{5}$$

where, in terms of the spatial momentum $\boldsymbol{p}$ of H_c in the H_b rest frame,

$$k \equiv M\sqrt{\frac{\boldsymbol{p}^2}{t}} = \sqrt{\frac{(t_+ - t)(t_- - t)}{4t}}, \tag{6}$$

in which we have, in turn, introduced two important kinematic values, $t_\pm \equiv (M \pm m)^2$.

B. $B \to D^*$, $B_s \to D_s^*$, $B_c^+ \to J/\psi$

Transition form factors of a pseudoscalar meson H_b to a vector meson H_c have been parametrized in a variety of ways in the literature. Here, we begin with a set [40] of vector $[V(t)]$ and axial-vector $[A_i(t)]$ form factors frequently used in lattice-QCD and model calculations,

$$\langle H_c(p, \epsilon)|(V - A)^\mu|H_b(P)\rangle \\ = \frac{2i\epsilon^{\mu\nu\rho\sigma}}{M + m} \epsilon_\nu^* p_\rho P_\sigma V(t) - (M + m)\epsilon^{*\mu}A_1(t) \\ + \frac{\epsilon^* \cdot q}{M + m}(P + p)^\mu A_2(t) + 2m\frac{\epsilon^* \cdot q}{q^2} q^\mu A_3(t) \\ - 2m\frac{\epsilon^* \cdot q}{q^2} q^\mu A_0(t), \tag{7}$$

where $q^\mu \equiv (P - p)^\mu$. Only four of these five form factors are independent; demanding that only $A_0(t)$ couples to timelike virtual W polarizations ($\propto q^\mu$) requires

$$A_3(t) = \frac{M + m}{2m} A_1(t) - \frac{M - m}{2m} A_2(t). \tag{8}$$

Requiring the cancellation of $1/q^2$ terms in Eq. (7) as $q^2 = t \to 0$ imposes the additional constraint $A_3(0) = A_0(0)$.

A different decomposition, in which the virtual W and vector meson H_c are described by their helicity states, turns out to be more useful for the dispersive analysis. Here, one exchanges the form factors V, A_0, A_1, A_2 for the set $g, f, \mathcal{F}_1, \mathcal{F}_2$. They are related by

$$g = \frac{2}{M + m}V,$$

$$f = (M + m)A_1,$$

$$\mathcal{F}_1 = \frac{1}{m}\left[-\frac{2k^2 t}{M + m}A_2 - \frac{1}{2}(t - M^2 + m^2)(M + m)A_1\right],$$

$$\mathcal{F}_2 = 2A_0. \tag{9}$$

$\mathcal{F}_{1,2}$, are proportional to the conventionally defined [41] helicity amplitudes $H_{0,t}$, respectively, while the other two helicity amplitudes $H_\pm$ are linear combinations of V and A form factors, $H_\pm(t) = f(t) \mp k\sqrt{t}g(t)$, where k is defined in Eq. (6).

At $t = t_-$, the middle two expressions of Eqs. (9) reduce to an additional constraint, $\mathcal{F}_1(t_-) = (M - m)f(t_-)$. In this basis, the previously noted constraint $A_3(0) = A_0(0)$ becomes $\mathcal{F}_1(0) = \frac{1}{2}(M^2 - m^2)\mathcal{F}_2(0)$. The differential decay rate for the semileptonic decay in this basis reads

$$\frac{d\Gamma}{dt} = \frac{G_F^2 |V_{cb}|^2}{192\pi^3 M^3} \frac{k}{t^{5/2}} (t - m_\ell^2)^2 \{(2t + m_\ell^2)[2t|f|^2 \\ + |\mathcal{F}_1|^2 + 2k^2 t^2|g|^2] + 3m_\ell^2 k^2 t|\mathcal{F}_2|^2\}. \tag{10}$$

C. $\Lambda_b \to \Lambda_c$

In the case of heavy-baryon transitions, the states of the spin-$\frac{1}{2}$ baryons are represented by spinors $u_{b,c}$. Here, there are two form factors for both the vector and axial-vector currents,

$$\langle \Lambda_c(p)|V^\mu|\Lambda_b(P)\rangle = \bar{u}_c(p)[F_1\gamma^\mu + F_2 v^\mu + F_3 v'^\mu]u_b(P),$$

$$\langle \Lambda_c(p)|A^\mu|\Lambda_b(P)\rangle = \bar{u}_c(p)[G_1\gamma^\mu + G_2 v^\mu + G_3 v'^\mu]\gamma_5 u_b(P), \tag{11}$$

where the kinematical variables relevant to the heavy-quark limit (see Sec. III) are the baryon 4-velocities, $v^\mu \equiv P^\mu/M_{\Lambda_b}$ and $v'^\mu \equiv p^\mu/M_{\Lambda_c}$. The differential decay rate is then

$$\frac{d\Gamma}{dt} = \frac{G_F^2 |V_{cb}|^2}{192\pi^3 M^3} \frac{k}{t^{5/2}} (t - m_\ell^2)^2 \{(t_- - t)(2t + m_\ell^2)[2t|F_1|^2 + |H_V|^2] + 3m_\ell^2(t_+ - t)|F_0|^2 \\ + (t_+ - t)(2t + m_\ell^2)[2t|G_1|^2 + |H_A|^2] + 3m_\ell^2(t_- - t)|G_0|^2\}, \tag{12}$$

where the form factors in the helicity basis read

$$H_V = (M + m)F_1 + \frac{1}{2}(t_+ - t)\left(\frac{F_2}{M} + \frac{F_3}{m}\right),$$

$$H_A = (M - m)G_1 - \frac{1}{2}(t_- - t)\left(\frac{G_2}{M} + \frac{G_3}{m}\right),$$

$$F_0 = (M - m)F_1 + \frac{1}{2M}(t + M^2 - m^2)F_2,$$

$$- \frac{1}{2m}(t - M^2 + m^2)F_3,$$

$$G_0 = (M + m)G_1 - \frac{1}{2M}(t + M^2 - m^2)G_2,$$

$$+ \frac{1}{2m}(t - M^2 + m^2)G_3. \tag{13}$$

As in the meson case, these form factors satisfy exact constraints at special kinematic points. Specifically, $H_A(t_-) = (M - m)G_1(t_-)$, $(M + m)F_0(0) = (M - m)H_V(0)$, and $(M - m)G_0(0) = (M + m)H_A(0)$. This basis differs from that used in the lattice-QCD calculations of Ref. [30] only by mass-dependent prefactors:

$$F_0 = (M - m)f_0^{\text{lat}},$$

$$H_V = (M + m)f_+^{\text{lat}},$$

$$F_1 = f_\perp^{\text{lat}},$$

$$G_0 = (M + m)g_0^{\text{lat}},$$

$$H_A = (M - m)g_+^{\text{lat}},$$

$$G_1 = g_\perp^{\text{lat}}. \tag{14}$$

III. HEAVY-QUARK SYMMETRIES

The physics of heavy-light hadrons ($Q\bar{q}$ or $Q\bar{q}\bar{q}'$) is simplified by the emergence of additional symmetries in the limit $m_Q \to \infty$. Operators distinguishing between heavy quarks of different spin orientation and flavor are suppressed by $1/m_Q$ and produce a vanishingly small effect upon physical amplitudes in the heavy-quark limit. All transition form factors between two hadrons with a single heavy quark and the same light-quark content are proportional to a single, universal Isgur-Wise function, $\xi(w)$ [42,43] for mesons or $\zeta(w)$ for baryons [44]. They are naturally expressed as w, which is the dot product of the initial and final heavy-light hadron 4-velocities, $v^\mu \equiv P^\mu/M$ and $v'^\mu \equiv p^\mu/m$, respectively, and fully contains the information about t:

$$w \equiv v \cdot v' = \gamma_m = \frac{E_m}{m} = \frac{M^2 + m^2 - t}{2Mm}. \tag{15}$$

The zero-recoil point, where the final hadron m is created at rest in the rest frame of the initial hadron M, satisfies $t = t_- \equiv (M - m)^2$, corresponding to $w = 1$. From the middle expressions of Eq. (15), one notes that w is the

Lorentz factor γ_m of m in the M rest frame. The maximum value of w in a given semileptonic process occurs when the momentum transfer t through the virtual W to the lepton pair—the total energy squared of the leptons in their rest frame—assumes its smallest possible value, $t = m_\ell^2$.

Heavy-quark symmetry encodes a physical picture in which a heavy-light hadron is described by a nearly static color-fundamental source with spin-independent interactions (the heavy quark Q), to which the matter associated with light degrees of freedom (light-quarks and gluons) is bound. In weak decays with $Q \to Q'$, the zero-recoil (Isgur-Wise) point corresponds to a situation in which Q spontaneously transforms to Q' at rest, but the decay otherwise leaves the light degrees of freedom undisturbed. The overlap between the initial and final light-quark wave functions is complete, so that $\xi(1) = 1$ or $\zeta(1) = 1$ at the zero-recoil (Isgur-Wise) point. Thus, in the heavy-quark limit, one obtains an absolute normalization for the form factors; in the meson case [37,42,43], all the form factors are proportional to $\xi(w)$,

$$f_+ = \frac{1}{2}\mathcal{F}_2 = \frac{1 + r}{2\sqrt{r}}\xi,$$

$$f_0 = \mathcal{F}_1 = M^2\sqrt{r}(1 - r)(1 + w)\xi,$$

$$g = \frac{1}{M\sqrt{r}}\xi,$$

$$f = M\sqrt{r}(1 + w)\xi, \tag{16}$$

while in the baryon case [44], all the form factors are proportional to $\zeta(w)$,

$$F_0 = H_A = M(1 - r)\zeta,$$

$$F_1 = G_1 = \zeta,$$

$$H_V = G_0 = M(1 + r)\zeta, \tag{17}$$

where $r \equiv m/M$. All of these results are corrected by effects of $\mathcal{O}(\Lambda_{\text{QCD}}/m_{Q'})$.

Due to the lack of lattice data for g, $\mathcal{F}_1$, and $\mathcal{F}_2$, we use the relations of Eq. (16) for f_+, f_0, and f to obtain $\xi_{(s)}(w)$ for each of the $B_{(s)} \to D_{(s)}$ processes from the existing lattice data. To establish a first approximation for an allowed region, we parametrize $\xi_{(s)}(w)$ by

$$\xi_{(s)}(w) = \xi_{(s)}(1) - \rho^2(w - 1) + \frac{1}{2}\sigma^2(w - 1)^2. \tag{18}$$

In our analysis, we have included an additional systematic error of 20% to account for violations of Isgur-Wise scaling. We sample three synthetic points from $\xi_{(s)}(w)$ for each form factor. For $B \to D$, the synthetic points are restricted to the same range $w < 1.16$ for $B \to D$ as the lattice data. For $B_s \to D_s$, where lattice results have been computed in the full w range, we restrict the synthetic points to the near-zero-recoil range of $w < 1.04$.

In decays of the types $B_c^+ \to J/\psi(\eta_c)\ell^+\nu_\ell$, the spectator c quark can no longer be considered light (and indeed is the same species as the final heavy quark). These cases are more complicated; the heavy-quark limit differs from the heavy-light case in two important ways [45]. First, the heavy-quark kinetic-energy operators for $\bar{b}$ and $\bar{c}$ quarks, while both scaling as $1/m_Q^{(\prime)}$, differ for the two flavors (thus breaking the heavy-quark flavor symmetry) but still provide leading-order corrections to the dynamics of the state due to the presence of the heavy spectator c; e.g., the Bohr radii of B_c and $J/\psi(\eta_c)$ are significantly different. Second, the spectator c receives a momentum transfer due to the transition $\bar{b} \to \bar{c}$ of the same order as the momentum imparted to the $\bar{c}$. Thus, the heavy-flavor symmetry due to the replacement of $\bar{b}$ with $\bar{c}$ does not leave the spectator degrees of freedom invariant, meaning that one cannot obtain a normalization of the form factors at the zero-recoil point based purely upon symmetry.

Even though the heavy-flavor symmetry obtained from replacing $\bar{b}$ with $\bar{c}$ is lost, the $\bar{b}$ and $\bar{c}$ quarks retain separate heavy-quark spin symmetries, as does the heavy spectator c. In addition, since the valence quarks are heavy, these systems are better described using nonrelativistic dynamics than are heavy-light systems. Indeed, $w_{\max} \approx 1.3$ for $B_c^+ \to J/\psi(\eta_c)$, a sufficiently modest value that suggests information obtained near the zero-recoil point remains phenomenologically useful. The six meson form factors of Eqs. (2) and (9) are related by the spin symmetries to a single, universal function that Ref. [45] calls Δ and Ref. [46] calls h. However, as emphasized in Ref. [45], the form factors only approach $\Delta(w)$ near the zero-recoil point, and its normalization there is not fixed by symmetry to assume a special value, like $\xi(1) = 1$.

A central feature of Ref. [45] is the use of the trace formalism of Ref. [47] to compute the relative normalization between the six meson form factors (i.e., to obtain the correct multiple of Δ for each tensor structure) near the zero-recoil point. To be specific, "near" in this sense means kinematic configurations in which the spatial momentum transfer to the spectator q is no larger than its mass m_q. This calculation was generalized in Refs. [46,48] using nonrelativistic QCD (NRQCD) to consider a small-recoil limit ($w \to 1$) in which the 4-velocities of $\bar{b}$ and $\bar{c}$ are nevertheless unequal (i.e., the spectator receives a momentum transfer at leading order in NRQCD). These relations were used in Refs. [25,32,33] to constrain the $B_c^+ \to J/\psi(\eta_c)$ form factors at zero recoil.

In this work, we extend the relations of Refs. [46,48] by deriving the leading-order NRQCD relations between the form factors and Δ at nonzero recoil. While these relations are expected to receive large corrections away from $w = 1$, we use them to construct ratios of derivatives of form factors at $w = 1$. To proceed, we start with the trace formalism of Ref. [47],

$$\langle\{J/\psi, \eta_c\}|\bar{b}\Gamma c|B_c^+\rangle$$
$$= -\sqrt{Mm}\mathrm{Tr}\left[\frac{1+\slashed{v}_{cs}}{2}B_c^+\gamma_5\frac{1-\slashed{v}_b}{2}\Gamma\right.$$
$$\left.\times\frac{1-\slashed{v}_c}{2}(J/\psi^{\dagger\mu}\gamma_\mu + \eta_c^\dagger\gamma_5)\right]\Delta, \qquad (19)$$

where v_{cs}, v_b, and v_c are the velocities of the spectator c quark, decaying b quark, and final-state c quark, respectively. These velocities are related in the heavy-quark limit to those of the mesons by $v_b \to \tilde{v}_1$, $v_c \to \tilde{v}_2$, and $v_{cs} \to -\tilde{v}_3 = \frac{1}{2}(v_1 + v_2)$, where

$$\tilde{v}_1^\mu = v_1^\mu + \theta(v_1 - v_2)^\mu, \quad \tilde{v}_2^\mu = v_2^\mu + \omega(v_2 - v_1)^\mu, \quad (20)$$

with $\theta \equiv \frac{m_3}{2m_1}$ and $\omega \equiv \frac{m_3}{2m_2}$. One can then use the trace formalism to obtain the w-dependent generalizations of the constants defined in Refs. [46,48]. Starting with the tensor definitions

$$\langle\eta_c(v_2)|V^\mu|B_c^+(v_1)\rangle \equiv \sqrt{m_{\eta_c}m_{B_c}}(c_1^P v_1^\mu + c_2^P v_2^\mu)\Delta,$$
$$\langle J/\psi(v_2)|V^\mu|B_c(v_1)\rangle \equiv \sqrt{m_{J/\psi}m_{B_c}}ic_V\epsilon^{\mu\nu\alpha\beta}\epsilon^{*\mu}v_{1\alpha}v_{2\beta}\Delta,$$
$$\langle J/\psi(v_2)|A^\mu|B_c(v_1)\rangle \equiv \sqrt{m_{J/\psi}m_{B_c}}[c_\epsilon\epsilon^{*\mu} + c_1(\epsilon^* \cdot v_1)v_1^\mu$$
$$+ c_2(\epsilon^* \cdot v_2)]\Delta, \qquad (21)$$

where

$$c_1^P = 1 + \theta - \omega - \frac{\omega}{2}(1 + \theta)(w - 1),$$
$$c_2^P = 1 - \theta + \omega - \frac{\theta}{2}(1 + \omega)(w - 1),$$
$$c_V = -1 - \theta - \omega,$$
$$c_\epsilon = 2 - \frac{\omega + \theta + 2\theta\omega - 2}{2}(w - 1),$$
$$c_1 = \frac{(3 + 2\theta)\omega}{2},$$
$$c_2 = -1 - \frac{\omega}{2} - \theta(1 + \omega), \qquad (22)$$

we construct the Isgur-Wise-like relations for the heavy-heavy systems:

$$f_+ = \sqrt{r}\frac{c_1^P + c_2^P r^{-1}}{2}\Delta,$$
$$f_0 = M^2\sqrt{r}[(1 - wr)c_1^P + (w - r)c_2^P]\Delta,$$
$$g = -\frac{c_V}{M\sqrt{r}}\Delta,$$
$$f = M\sqrt{r}c_\epsilon\Delta,$$
$$\mathcal{F}_1 = M^2\sqrt{r}[(w - r)c_\epsilon + (rc_1 + c_2)(w^2 - 1)]\Delta,$$
$$\mathcal{F}_2 = \frac{c_\epsilon + (1 - wr)c_1 + (w - r)c_2}{\sqrt{r}}\Delta. \qquad (23)$$

These relations reproduce the standard Isgur-Wise results [37,42,43] of Eq. (16) in the limit θ, $\omega \to 0$, and

they reduce to the relations of Refs. [46,48] when $w \to 1$. Terms that break these relations should be $\mathcal{O}(m_c/m_b, \Lambda_{QCD}/m_c) \approx 30\%$, and in our analysis, we conservatively allow for up to 50% violations. We use these relations in our analysis to fix both the relative normalization between form factors and their slopes at zero recoil. These results are obtained by constructing ratios from Eq. (23) after solving for $\Delta(w = 1)$ and $d\Delta/dw|_{w=1}$.

IV. LATTICE QCD RESULTS

This work uses the existing lattice-QCD results for $b \to c$ form factors as input to our global analysis. These results have been produced by a number of different groups, and the determinations of the various form factors have been performed at varying numbers of momentum-transfer values t and with varying treatments of uncertainties. In this section, we summarize the lattice results used in our analysis.

The best current results are those for $B \to D$ form factors. The form factors f_+ and f_0 have been computed by two groups [27,28], including a complete treatment of all sources of error. We use the results of Ref. [28] alone in the final results, having found that the larger uncertainties of Ref. [27] mean that they provide no significant additional constraint.

For the case of $B_s \to D_s$, a single group has produced results for f_+ and f_0 at nonzero recoil with a complete error treatment [29]. The baryonic process $\Lambda_b \to \Lambda_c$ has been computed in Ref. [30] on only one lattice volume, but their results include a 1.5% systematic uncertainty for finite-volume effects, and given a quantified error estimate, we can include these lattice data in our analysis.

The heavy-heavy process $B_c^+ \to \eta_c$ has also only been computed by one group [39], with an incomplete treatment of errors. It was computed on a single lattice volume, so finite-volume effects are potentially worrying. To account for possible large finite-volume effects, in the analysis, we included an additional 20% systematic error.

In the process $B_c^+ \to J/\psi$, the two form factors g and f have been reported at nonzero recoil by one group on one lattice volume [39]. For these form factors, we also include an additional 20% systematic error. For the other two form factors, $\mathcal{F}_1$ and $\mathcal{F}_2$, no results have been presented.

For the final two processes $B \to D^*$ and $B_s \to D_s^*$, only the zero-recoil value of f [which is exactly related to $\mathcal{F}_1$ at zero recoil; see above Eq. (10)] has been computed. In the case of $B \to D^*$, $f(t_-)$ has been computed by two groups [49,50], and here we take the FLAG value [26]. For $B_s \to D_s^*$, we include the recent result of Ref. [51]. In addition to the lack of nonzero recoil data, no results for g and $\mathcal{F}_2$ at any points are available.

The presentation of these results in the literature is also varied. For some, only a functional form is presented; in such cases, we resample the form factors at a fixed number of t values, using the full error estimates and correlation matrices. Other form factors are presented at fixed values of t; in such cases, we sample the form factors at the given t values.

V. DISPERSIVE RELATIONS

This work employs the model-independent form-factor parametrization of BGL [37,38], which rests on the twin principles of analyticity and unitarity of particular two-point Green's functions. While originally applied to the form factors of heavy-light semileptonic decays, this parametrization was extended to heavy-heavy systems in Refs. [25,32] (using a slightly different set of free parameters to simplify the computation). The essential ingredients are summarized here.

The two-point momentum-space Green's function $\Pi_J^{\mu\nu}$ of a vectorlike quark current, $J^\mu \equiv \bar{Q}\Gamma^\mu Q'$, can be expanded in a variety of ways [36,37,52–54]. For our purpose, it is convenient is to break $\Pi_J^{\mu\nu}$ into spin-1 (Π_J^T) and spin-0 (Π_J^L) pieces [37]. The functions $\Pi_J^{L,T}$ are divergent in perturbative QCD (pQCD) and require subtractions in order to be rendered finite. After performing the minimum necessary numbers of subtractions for each function, one obtains the finite dispersion relations:

$$\chi_J^L(q^2) \equiv \frac{\partial \Pi_J^L}{\partial q^2} = \frac{1}{\pi} \int_0^\infty dt \frac{\operatorname{Im} \Pi_J^L(t)}{(t - q^2)^2},$$

$$\chi_J^T(q^2) \equiv \frac{1}{2} \frac{\partial^2 \Pi_J^T}{\partial(q^2)^2} = \frac{1}{\pi} \int_0^\infty dt \frac{\operatorname{Im} \Pi_J^T(t)}{(t - q^2)^3}. \quad (24)$$

Since q^2 remains as a free parameter in these equations, one may select its value in order to obtain the tightest possible phenomenological constraints (which requires that q^2 is as close to the region of hadronic masses as possible) but still require that $\chi_J(q^2)$ can be computed to good accuracy using pQCD (the asymptotic regime of which is the deep-Euclidean limit, $q^2 \to -\infty$). The parametric requirement for the latter condition is $(m_Q + m_{Q'})\Lambda_{QCD} \ll (m_Q + m_{Q'})^2 - q^2$, which is clearly satisfied by $q^2 = 0$ for any process in which either or both of Q, Q' is heavy compared to Λ_{QCD}, as is true for all cases considered here. $\chi_J(q^2 = 0)$ has been computed to two-loop pQCD order, including leading nonperturbative vacuum condensates [21,55–59].

Unitarity requires that each of the functions $\operatorname{Im}\Pi_J$ admits an expansion over all hadronic states X that couple to the vacuum through the current J^μ:

$$\operatorname{Im} \Pi_J^{T,L}(q^2) = \frac{1}{2} \sum_X (2\pi)^4 \delta^4(q - p_X) |\langle 0|J|X\rangle|^2. \quad (25)$$

Since every nontrivial term in Eq. (25) is positive, one may truncate the sum on X after any number of states, insert the sum into Eq. (24), and obtain a strict inequality based upon unitarity. While typically these inequalities have been

employed for single states X, they clearly become stronger when more states X are included [6,23,37], which is a key ingredient of our analysis here. Our set of X includes only below-threshold $B_c^{(*)}$ poles and the two-body channels discussed above. Additional branch points corresponding to the thresholds of processes such as $B_c \pi \pi$ occur at lower t values, but their contributions to the dispersive bounds are expected to be small due to OZI suppression, closeness to the $B^{(*)}D$ thresholds that are already taken into account, or both.

For the purposes of this work, the first physically significant two-body production threshold occurs at $t = t_{bd} \equiv (M_{B^{(*)}} + M_D)^2$, depending upon which component of the two-point function is being considered (see Table II). t_{bd} thereby represents the lowest significant branch point in the two-point function.

Analyticity properties of the Green's function are incorporated by a conformal mapping of the complex-t plane with a cut beginning at the branch point $t = t_*$ to the unit disk in a complex variable z,

$$z(t; t_0) \equiv \frac{\sqrt{t_* - t} - \sqrt{t_* - t_0}}{\sqrt{t_* - t} + \sqrt{t_* - t_0}}; \qquad (26)$$

the two edges of the branch cut in t are mapped to the unit circle C in z. The parameter t_0 is free at this stage; we later optimize this choice [Eqs. (31)–(32)] to improve the convergence of the Green's function in the variable z.

The importance of allowing a branch point t_* that does not necessarily equal t_+ becomes apparent in processes for which t_+ lies well above the lowest significant branch point for the two-point function. Such an effect is especially significant for baryon decays such as $\Lambda_b \to \Lambda_c$ and $\Lambda_b \to p$. Previous studies that automatically set $t_* = t_+$ [37,53] can introduce branch cuts [e.g., for $B^{(*)}D^{(*)}$ pairs] inside the unit circle C defined by $|z| = 1$. The purpose of the BGL parametrization being to eliminate all significant nonanalytic behavior below t_*, there are two choices: either model the strength of the branch cut (which requires both knowledge of the branch point and the function along the cut) and use this information to loosen the strength of the bounds, or instead set $t_* = t_{bd}$ (as is done here). With this latter choice, $t_* < t_+$ is no longer the threshold relevant to

the physical process, but it is the location of an important branch cut in the two-point function to which the process contributes. Nevertheless, for all heavy-quark systems, one finds that the semileptonic decay region $m_\ell^2 \leq t \leq t_-$ lies substantially below t_{bd}, and therefore the BGL bounds are not strongly affected.

With this choice, the bounds obtained by inserting Eq. (25) into Eq. (24) amount to an integral over the unit circle $|z| = 1$ of an integrand containing the form factor F_i of interest multiplied by the known *outer functions* $\phi_i(t; t_0)$, which incorporate information about kinematics and changes of variable. (These functions are tabulated for the cases of interest in Refs. [25,32].) The only significant nonanalytic features remaining within the unit circle $|z| = 1$ are simple poles corresponding to $B_c^{(*)}$ states. Each such pole at a known location $t = t_s$ can effectively be removed from the integrand through multiplication by $z(t; t_s)$ (a *Blaschke factor*). In the $b \to c$ processes of interest here, the masses corresponding to the $B_c^{(*)}$ poles that must be removed in this analysis are collected in Table II, organized by the J^P channel to which each one contributes ($1^-\{f_+, g, F_V, H_V\}$; $1^+\{f, \mathcal{F}_1, G_1, H_A\}$; $0^+\{f_0, F_0\}$; $0^-\{\mathcal{F}_2, G_0\}$). These masses have either been measured at the LHC [60,61] (boldface) or are derived from very recent model calculations [62].

Denoting the product of Blaschke factors for all poles with $|z| < 1$ as P_i, the unitarity bound for the form factor F_i expressed entirely in terms of the conformal variable z reads

$$\frac{1}{2\pi i} \sum_i \oint_C \frac{dz}{z} |\phi_i(z) P_i(z) F_i(z)|^2 \leq 1. \qquad (27)$$

Since the product $\phi_i(z) P_i(z) F_i(z)$ is an analytic function inside the unit circle $|z| = 1$, one may write

$$F_i(t) = \frac{1}{|P_i(t)| \phi_i(t; t_0)} \sum_{n=0}^{\infty} a_n^i z(t; t_0)^n. \qquad (28)$$

Inserting Eq. (28) into Eq. (27), one finds that the unitarity bound can be compactly written as a constraint on the Taylor-series coefficients a_n^i:

$$\sum_{i; n=0}^{\infty} (a_n^i)^2 \leq 1. \qquad (29)$$

Equations (28) and (29) are the essence of the BGL parametrization. Every functional form for $F_i(t)$ that respects analyticity and unitarity, as expressed by Eqs. (24) and (25), can be expressed in terms of a set of Taylor coefficients a_n^i that satisfy the sum rule Eq. (29).

As in Ref. [25], the generalization of the location of the branch point from t_+ to t_{bd} means that slightly more complicated functions of the mass parameters appear in the analysis. Reprising this previous notation, we define

TABLE II. All B_c-state masses lying below the thresholds $t = t_{bc}$ (for which "Lowest pair" indicates the states of which the masses enter into t_{bc}) for the J^P channels relevant to this study. Numbers in bold are masses measured at the LHC.

Type	J^P	Lowest pair	M (GeV)
Vector	1^-	BD	6.3290, 6.8975, 7.0065
Axial	1^+	B^*D	6.7305, 6.7385, 7.1355, 7.1435
Scalar	0^+	BD	6.6925, 7.1045
Pseudoscalar	0^-	B^*D	**6.2749(8)**, **6.8710(16)**

$$r \equiv \frac{m}{M}, \qquad \delta \equiv \frac{m_\ell}{M},$$

$$\beta \equiv \frac{M_{B^{(*)}}}{M}, \qquad \Delta \equiv \frac{M_D}{M},$$

$$\kappa \equiv (\beta + \Delta)^2 - (1 - r)^2,$$

$$\lambda \equiv (\beta + \Delta)^2 - \delta^2, \tag{30}$$

and the free parameter t_0 in Eq. (26) is replaced by a parameter N:

$$N \equiv \frac{t_{\rm bd} - t_0}{t_{\rm bd} - t_-}. \tag{31}$$

Computing the kinematical range for the semileptonic process given in terms of z is then straightforward. The minimal (optimized) truncation error is achieved when $z_{\min} = -z_{\max}$, which occurs when $N = N_{\rm opt} = \sqrt{\frac{\lambda}{\kappa}}$. At this point, one obtains

$$z_{\max} = -z_{\min} = \frac{\lambda^{1/4} - \kappa^{1/4}}{\lambda^{1/4} + \kappa^{1/4}}. \tag{32}$$

One finds that the semileptonic decay processes under consideration do not exceed $z_{\max} \approx 0.03$. If instead $t_{\rm bd}$ is set equal to t_+, then Eq. (30) reduce to $\Delta \to r$, $\beta \to 1$, and $\kappa \to 4r$, and all of the expressions reduce to those given in Ref. [38].

VI. RESULTS

The global analysis of the $b \to c$ hadronic form factors relies upon a number of constraints. They are summarized here for the convenience of the reader:

(i) The $n \leq 2$ coefficients a_n^i in each channel are constrained by $\sum_{n,i}(a_n^i)^2 \leq 1$ [Eq. (29)].

(ii) The form factors satisfy the exact kinematic relations below Eq. (3), above Eq. (10), and below Eq. (13)]:

$$\mathcal{F}_1(t_-) = M(1 - r)f(t_-),$$

$$\mathcal{F}_1(0) = \frac{1}{2}M^2(1 - r^2)\mathcal{F}_2(0),$$

$$f_+(0) = M^2(1 - r^2)f_0(0),$$

$$H_A(t_-) = M(1 - r)G_1(t_-),$$

$$M(1 + r)F_0(0) = M(1 - r)H_V(0)$$

$$M(1 - r)G_0(0) = M(1 + r)H_A(0). \tag{33}$$

(iii) $B_{(s)} \to D^*_{(s)}$ form factors are taken to be consistent with the form factor $\xi_{(s)}(w)$ derived from $B_{(s)} \to D_{(s)}$, once an additional 20% systematic error is included to account for violations of Isgur-Wise scaling.

(iv) $B_{(s)} \to D^*_{(s)}$ form factors are maximal at the zero-recoil point $t = t_-$, since the universal form factor $\xi_{(s)}$ represents an overlap matrix element between initial and final states. This condition is implemented via the constraints $F_i(t_-) \geq F_i(0)$ and $\frac{dF_i}{dt}\big|_{t_-} \geq 0$, where F_i represents any of the form factors.

(v) The normalizations and slopes of the $B_c^+ \to \{J/\psi, \eta_c\}$ form factors $f_+, g(\propto V), \mathcal{F}_1, \mathcal{F}_2$ are required to be consistent at zero recoil [via Eq. (23)] to within 50% with the results for f_0, $f(\propto A_1)$ computed from lattice QCD.

We perform the constrained multivariable fit by first randomly sampling q^2 values of the form factors for which lattice data are known. If correlations have been reported by the lattice QCD groups, they are implemented in the sampling. The preliminary HPQCD results for $B_c^+ \to \{J/\psi, \eta_c\}$ report only statistical error. To account for the unknown systematics like finite-volume and discretization effects, we include in quadrature an additional systematic error $f_{lat} = 20\%$ (as a percentage of the form factor at each point). Lines of best fit are then computed from the collection of sampled points using a least-squares procedure. The resulting form factors, exhibited with 1σ bands, are presented in Figs. 1–8. The a_n^i for the form factors can be found in Table III. Of particular note, our theoretical values for the form factors are consistent with those of the two processes $B \to D^{(*)}$ for which experimental data have been obtained [63–65].

In interpreting these 1σ bands, it is important to recall that this analysis includes statistical errors from the lattice studies for which the notion of "1σ" is well defined. However, the analysis also includes systematic errors for which, strictly speaking, it is not. Moreover, in assigning systematic error associated with limited lattice data for which systematic errors had not been carefully studied, or due to truncation errors in the theory, we have been quite
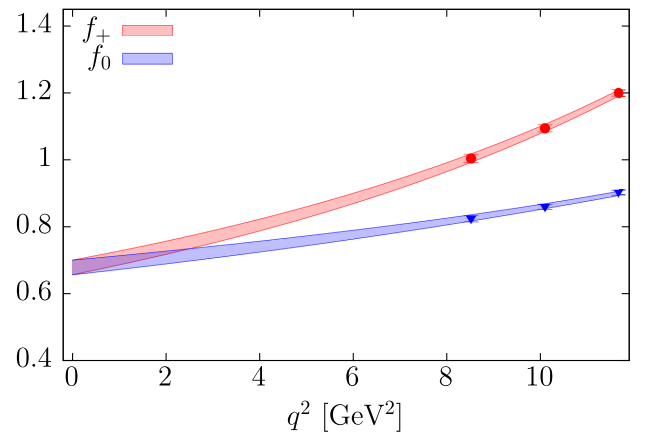

FIG. 1. $B \to D$ form factors: $f_+(q^2)$ (red circles) and $f_0(q^2)/M^2(1 - r^2)$ (blue triangles) from Ref. [28]. The colored bands are the one-standard-deviation (1σ) best-fit regions obtained from our global dispersive analysis.
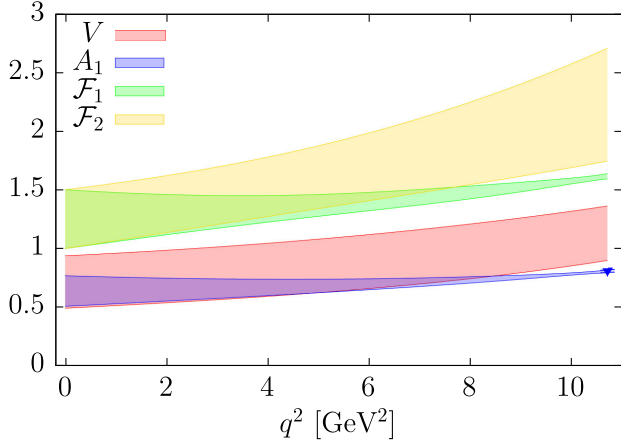
FIG. 2. $B \to D^*$ form factors: $A_1(q^2_{max})$ (blue triangle) from Ref. [26]. The colored bands are the one-standard-deviation (1σ) best-fit regions obtained from our global dispersive analysis. $\mathcal{F}_1$ has been divided by $\frac{1}{2}M^2(1-r^2)$.

FIG. 4. $B_s \to D^*_s$ form factors: $A_1(q^2_{max})$ (blue triangle) from Ref. [51]. The colored bands are the one-standard-deviation (1σ) best-fit regions obtained from our global dispersive analysis. $\mathcal{F}_1$ has been divided by $\frac{1}{2}M^2(1-r^2)$.

conservative. Thus, one might reasonably expect the SM result to fall within these bands with a higher probability than had the bands been entirely due to statistical errors.

From Table III, it is possible to investigate the convergence of BGL expansion. All the a_2 coefficients are consistent with zero at 1.2σ, suggesting that each series is rapidly converging; additional parameters are unnecessary at the present precision of lattice data. This lack of precision also allows for the a_2 parameters to fluctuate substantially, such that in a given fit each one can typically be $\mathcal{O}(0.1)$, and therefore contribute significantly to the dispersive bounds of Eq. (29).

With this observation, one would expect the dispersive bounds to be saturated, similar to the results of Ref. [25] in which the dispersive bound for the unknown form factor $\mathcal{F}_2$ was saturated. Fitting all seven processes together, Eq. (29) is typically saturated for all four channels (T, L; V, A). The saturation of the bounds is not due solely to the

ill-constraint of the a_2 parameters. Surprisingly, Table III shows that for the two $\Lambda_b \to \Lambda_c$ form factors F_0 and G_0 the a_1 coefficients are $\mathcal{O}(0.5)$. Each one of them saturates about 25% of the dispersive bound. This result suggests that the inclusion of baryonic channels into the dispersive approach is particularly powerful.

In the case of G_0, there are additional benefits beyond providing such a large contribution toward saturation. In the 0^- channel, only the G_0 and $\mathcal{F}_2$ form factors contribute. At present, no lattice results for any $\mathcal{F}_2$ exist. Given that $\mathcal{F}_2$ form factors contribute significantly only to τ decays, this uncertainty is a sizeable fraction of the uncertainty in our predictions of $R(H_c)$. The large contribution of G_0 to the dispersive bound reduces this error. These dual benefits from including $\Lambda_b \to \Lambda_c$ should motivate future efforts to obtain lattice results for form factors of other baryonic processes, i.e., $\Lambda_b \to \Lambda^*_c$.

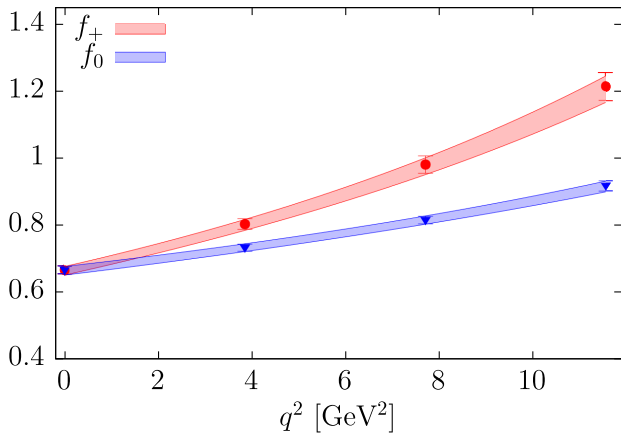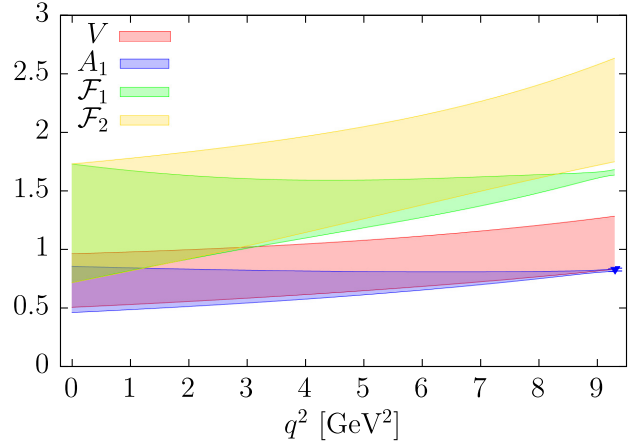
FIG. 3. $B_s \to D_s$ form factors: $f_+(q^2)$ (red circles) and $f_0(q^2)/M^2(1-r^2)$ (blue triangles) from Ref. [29]. The colored bands are the one-standard-deviation (1σ) best-fit regions obtained from our global dispersive analysis.
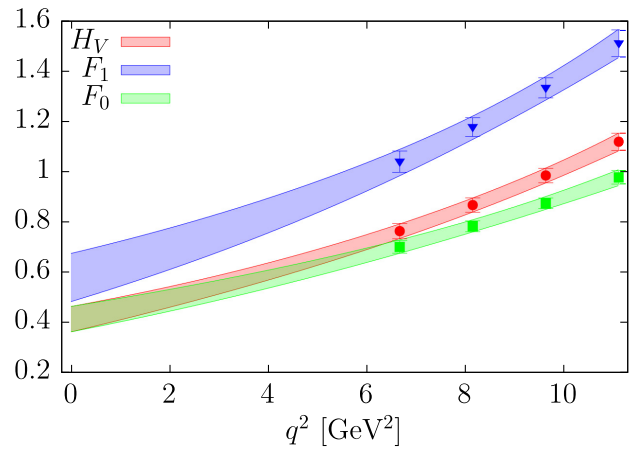

FIG. 5. $\Lambda_b \to \Lambda_c$ form factors: $H_V(q^2)/M(1+r)$ (red circles), $F_1(q^2)$ (blue triangles), and $F_0(q^2)/M(1-r)$ (green squares) from Ref. [30]. The colored bands are the one-standard-deviation (1σ) best-fit regions obtained from our global dispersive analysis.
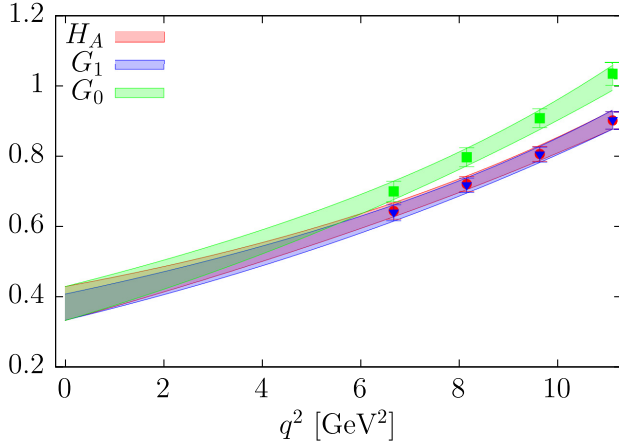
FIG. 6. $\Lambda_b \to \Lambda_c$ form factors: $H_A(q^2)/M(1-r)$ (red circles), $G_1(q^2)$ (blue triangles), and $G_0(q^2)/M(1+r)$ (green squares) from Ref. [30]. The colored bands are the one-standard-deviation (1σ) best-fit regions obtained from our global dispersive analysis.

In the case of $\Lambda_b \to \Lambda_c$, sufficient lattice data exist so that the constraint of heavy-quark symmetries is not required to fix the form factors. Therefore, we can use our results in that process to investigate how well the heavy quark effective theory (HQET) relations are satisfied. While higher-order terms are known [31], we consider the leading-order relations in which the six form factors are all proportional to an Isgur-Wise function $\zeta(w)$, which is typically expanded in powers of $w - 1$ as

$$\zeta(w) = \zeta(1) - \rho^2(w-1) + \frac{1}{2}\sigma^2(w-1)^2. \quad (34)$$

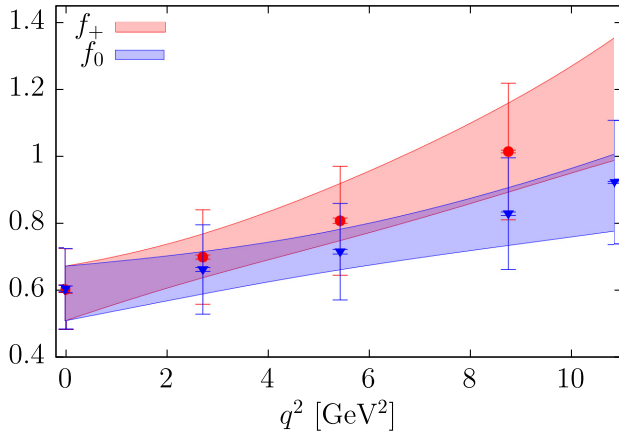In this expansion, our results for the coefficients of the Taylor series are found in Table IV. One can see that our

FIG. 7. $B_c^+ \to \eta_c$ form factors: $f_+(q^2)$ (red circles) and $f_0(q^2)/M^2(1-r^2)$ (blue triangles) from the HPQCD Collaboration [39]. The interior bars represent the statistical uncertainty quoted by HPQCD. The exterior bars represent the result of including our $f_{\text{lat}} = 20\%$ systematic uncertainty. The colored bands are the one-standard-deviation (1σ) best-fit regions obtained from our global dispersive analysis.

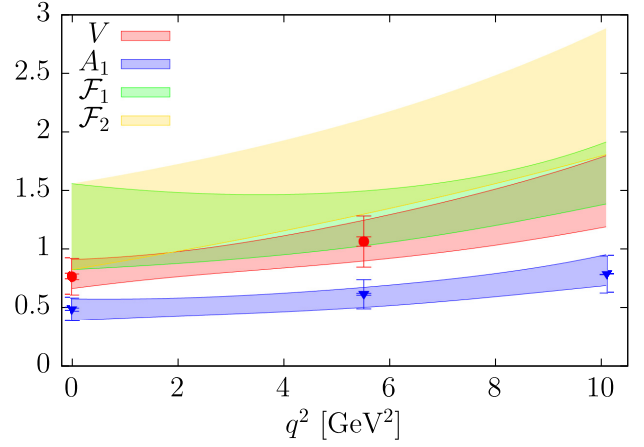FIG. 8. $B_c^+ \to J/\psi$ form factors: $V(q^2)$ (red circles) and $A_1(q^2)$ (blue triangles) from the HPQCD Collaboration [39]. The interior bars represent the statistical uncertainty quoted by HPQCD. The exterior bars represent the result of including our $f_{\text{lat}} = 20\%$ systematic uncertainty. The colored bands are the one-standard-deviation (1σ) best-fit regions obtained from our global dispersive analysis. $\mathcal{F}_1$ has been divided by $\frac{1}{2}M^2(1-r^2)$.

TABLE III. The BGL coefficients a_n^i of this $N = 2$ analysis. The full correlation matrix between the coefficients can be found in the supplemental material [66].

$b \to c$	F_i	a_0^i [$\times 10^2$]	a_1^i [$\times 10^2$]	a_2^i [$\times 10^2$]
$B \to D$	f_0	7.2(1.0)	−17.(4)	0.7(6)
	f_+	0.25(4)	−0.58(9)	1(14)
$B \to D^*$	g	0.67(17)	−0.5(14)	10(40)
	f	0.42(3)	−0.2(13)	20(30)
	$\mathcal{F}_1$	0.07(4)	−0.11(17)	1(7)
	$\mathcal{F}_2$	5.4(1.0)	−20(30)	−10(60)
$B_s \to D_s$	f_0	5.23(8)	−16(17)	1(4)
	f_+	0.179(5)	−0.47(9)	−1.6(5)
$B_s \to D_s^*$	g	0.46(11)	0(300)	16(16)
	f	0.33(4)	−0.4(20)	18(19)
	$\mathcal{F}_1$	0.05(6)	−0.2(4)	2(11)
	$\mathcal{F}_2$	4(9)	−20(30)	0(300)
$\Lambda_b \to \Lambda_c$	H_V	0.256(9)	−2.7(4)	2(7)
	F_1	0.85(4)	−7.9(1.7)	4(14)
	F_0	5.14(18)	−46(9)	1(3)
	H_A	0.0613(18)	−0.49(9)	−1(3)
	G_1	0.356(12)	−2.7(5)	−3(4)
	G_0	5.23(18)	−53(9)	1.3(1.2)
$B_c^+ \to \eta_c$	f_0	6.1(6)	−30(30)	10(70)
	f_+	0.18(3)	−0.8(7)	−3(15)
$B_c^+ \to J/\psi$	g	0.47(9)	−2(3)	20(60)
	f	0.34(5)	−2.6(2.0)	40(60)
	$\mathcal{F}_1$	0.058(10)	−0.3(3)	9(8)
	$\mathcal{F}_2$	4(10)	−21(16)	0.8(9)

TABLE IV.   HQET expansion parameters for $\Lambda_b \to \Lambda_c$ obtained from this analysis. ζ_{AVG} indicates the values of the Isgur-Wise function obtained by averaging all of the form factors, while $\zeta_{w \to 1}$ is obtained by averaging only over the form factors H_A and G_1 that contribute significantly at zero recoil.

$F_i(q^2)$	$F_i(1)$	ρ^2	σ^2
H_V	1.12(4)	2.5(3)	5.6(1.8)
F_1	1.51(7)	3.3(5)	8.0(1.8)
F_0	0.97(4)	1.8(3)	3.6(6)
H_A	0.90(3)	1.7(3)	3.4(1.8)
G_1	0.90(3)	1.82(18)	4.0(8)
G_0	1.02(4)	2.2(3)	4.8(6)
ζ_{AVG}	1.1(3)	2.2(7)	4(2)
$\zeta_{w \to 1}$	0.90(3)	1.7(2)	3.6(1.4)

results, despite suggesting corrections to the HQET relations, are consistent with the sum-rule bounds: $\rho^2 \geq 0$ and $\sigma^2 \geq \frac{3}{5}[\rho^2 + (\rho^2)^2]$ [67].

In the final two rows of Table IV, we compute a pair of averages of the coefficients. The first, ζ_{AVG}, is simply an average of parameters from all six form factors together and would represent a best-fit phenomenological value for $\zeta(w)$. The last row ($\zeta_{w \to 1}$) instead averages over only H_A and G_1. This average is of interest because only these two form factors contribute appreciably to the differential decay rate of $\Lambda_b \to \Lambda_c \mu^- \bar{\nu}_\mu$, the process measured by the LHCb Collaboration [68]. In that work, assuming the same leading-order HQET relations and the static approximation, LHCb extracted the values $\rho^2 = 1.63(11)$ and $\sigma^2 = 2.16(34)$ from the decay $\Lambda_b \to \Lambda_c \mu^- \bar{\nu}_\mu$. Good agreement is found between the LHCb results and those of ζ_{AVG}. But if these results were used to make predictions far from $w \to 1$, or for $\Lambda_b \to \Lambda_c \tau^- \bar{\nu}_\tau$, then the other form factors would begin to contribute appreciably, and a systematic error would be introduced because their corresponding coefficients differ dramatically from those of $\zeta_{w \to 1}$.

Using the computed form factors, we extract three observables of experimental interest and present the results in Table V. The first is the semileptonic decay ratio:

TABLE V.   Results of our dispersive analysis for the semileptonic decay ratio $R(H_c)$, τ polarization $P_\tau(H_c)$, and the (vector) H_c polarization fraction $F_L^{H_c}$.

$b \to c$	$R(H_c)$	$P_\tau(H_c)$	$F_L^{H_c}$
$B \to D$	0.298(6)	0.325(4)	$\cdots$
$B \to D^*$	0.252(14)	$-0.51(5)$	0.45(3)
$B_s \to D_s$	0.300(5)	0.323(18)	$\cdots$
$B_s \to D_s^*$	0.20(3)	$-0.49(5)$	0.44(5)
$\Lambda_b \to \Lambda_c$	0.332(10)	$-0.308(15)$	$\cdots$
$B_c^+ \to \eta_c$	0.30(5)	0.33(11)	$\cdots$
$B_c^+ \to J/\psi$	0.25(3)	$-0.47(5)$	0.46(4)

$$R(H_c) = \frac{\Gamma(H_b \to H_c \tau \nu_\tau)}{\Gamma(H_b \to H_c \mu \nu_\mu)}. \tag{35}$$

For those $R(H_c)$ for which existing theoretical values exist, we find good agreement, including predictions that make further, model-dependent assumptions (e.g., Ref. [69]). This result is to be expected, given that all the theoretical values rely at least in part upon the same lattice-QCD data used here. Beyond these checks, we have produced two new SM predictions, those of $R(J/\psi) = 0.25(3)$ and $R(D_s^*) = 0.20(3)$, which can be compared to the upcoming LHCb results of runs II and III. We find that the $R(J/\psi)$ prediction is within 1.8σ of the current LHCb result of $0.71(17)(18)$ [24].

The second observable is the polarization of the τ lepton, given by

$$P_\tau(H_c) \equiv \frac{\Gamma^+ - \Gamma^-}{\Gamma^+ + \Gamma^-}, \tag{36}$$

where $\Gamma^\pm$ are the decay rates of a τ with fixed helicity $\lambda = \pm$. Only $P_\tau(D^*) = -0.38(60)$ has been measured [16,19], and our value $-0.51(15)$ agrees within uncertainties. For the other processes, we present predictions for comparison with future measurements.

The final observable we compute is the fractional longitudinal polarization of the decaying vector meson,

$$F_L^{H_c} \equiv \frac{\Gamma^0}{\Gamma}, \tag{37}$$

where Γ^0 is the decay rate of a vector H_c with helicity $\lambda = 0$. In the case of the D^*, this quantity has been measured to be $F_L^{D^*} = 0.60(9)$ [70], which is within 1.6σ of our result and other existing SM values [7,71].

VII. DISCUSSION AND CONCLUSION

In this work, we have presented model-independent predictions of the $b \to c$ hadronic transition form factors for the processes $B \to \{D, D^*\}$, $B_s \to \{D_s, D_s^*\}$, $B_c \to \{J/\psi, \eta_c\}$, and $\Lambda_b \to \Lambda_c$ using a coupled global analysis. From these form factors, Standard Model values for $R(H_c)$ (τ-μ ratio), $P_\tau(H_c)$ (τ polarization), and $F_L^{H_c}$ (H_c longitudinal component) were computed. Also obtained, for the first time using this approach, were $R(D_s^*) = 0.20(3)$ and $R(J/\psi) = 0.25(3)$. The near-term outlook for higher-statistics measurements from BELLE and LHCb, coupled with new lattice results, promise to reduce the uncertainty on the experimental and theoretical values dramatically, allowing for a refinement of the investigation of the beyond-SM contributions to charged currents (e.g., Refs. [72,73]). Additionally, new measurements like $R(D_s^{(*)})$ can be compared to our results to provide complementary constraints.

We have also derived nonzero-recoil relations between the heavy-heavy meson form factors $B_c \to \{J/\psi, \eta_c\}$ and the Isgur-Wise-like form factor Δ at leading order in NRQCD. These results allow constraints on the slopes of unknown lattice form factors at $w = 1$ to be obtained. Furthermore, these relations can be used as the basis of phenomenological models for the form factors.

The dominant sources of uncertainty in this analysis arise from the form factors for which no lattice data have been reported, all of which are in the $P \to V$ processes. Upcoming results for $B \to D^*$ [74] and $B_c^+ \to J/\psi$ promise to provide insight into these form factors. The global analysis could also benefit from the inclusion of new processes. Given the large fractional saturation of the unitarity bounds by $\Lambda_b \to \Lambda_c$, the inclusion of $\Lambda_b \to \Lambda_c^*$ could be particularly fruitful once such data are available.

ACKNOWLEDGMENTS

[1] P. Colangelo and F. De Fazio, J. High Energy Phys. 06 (2018) 082.

[2] M. A. Ivanov, J. G. Körner, and C.-T. Tran, Phys. Rev. D **94,** 094028 (2016).

[3] C.-T. Tran, M. A. Ivanov, J. G. Körner, and P. Santorelli, Phys. Rev. D **97,** 054014 (2018).

[4] S. Bhattacharya, S. Nandi, and S. K. Patra, Phys. Rev. D **93,** 034011 (2016).

[5] S. Bhattacharya, S. Nandi, and S. K. Patra, Phys. Rev. D **95,** 075012 (2017).

[6] S. Jaiswal, S. Nandi, and S. K. Patra, J. High Energy Phys. 12 (2017) 060.

[7] S. Bhattacharya, S. Nandi, and S. Kumar Patra, Eur. Phys. J. C **79,** 268 (2019).

[8] T. D. Cohen, H. Lamm, and R. F. Lebed, Phys. Rev. D **98,** 034022 (2018).

[9] D. Bečirević, M. Fedele, I. Nišandžić, and A. Tayduganov, arXiv:1907.02257.

[10] J. P. Lees *et al.* (BABAR Collaboration), Phys. Rev. Lett. **109,** 101802 (2012).

[11] J. P. Lees *et al.* (BABAR Collaboration), Phys. Rev. D **88,** 072012 (2013).

[12] M. Huschle *et al.* (Belle Collaboration), Phys. Rev. D **92,** 072014 (2015).

[13] A. Abdesselam *et al.* (Belle Collaboration), arXiv:1904.08794.

[14] Y. Sato *et al.* (Belle Collaboration), Phys. Rev. D **94,** 072007 (2016).

[15] R. Aaij *et al.* (LHCb Collaboration), Phys. Rev. Lett. **115,** 111803 (2015); **115,** 159901(E) (2015).

[16] S. Hirose *et al.* (Belle Collaboration), Phys. Rev. Lett. **118,** 211801 (2017).

[17] R. Aaij *et al.* (LHCb Collaboration), Phys. Rev. Lett. **120,** 171802 (2018).

[18] R. Aaij *et al.* (LHCb Collaboration), Phys. Rev. D **97,** 072013 (2018).

[19] S. Hirose *et al.* (Belle Collaboration), Phys. Rev. D **97,** 012004 (2018).

[20] Y. Amhis *et al.* (Heavy Flavor Averaging Group), Eur. Phys. J. C **77,** 895 (2017), updated results and plots available at https://hflav.web.cern.ch.

[21] D. Bigi and P. Gambino, Phys. Rev. D **94,** 094008 (2016).

[22] F. U. Bernlochner, Z. Ligeti, M. Papucci, and D. J. Robinson, Phys. Rev. D **95,** 115008 (2017); **97,** 059902(E) (2018).

[23] D. Bigi, P. Gambino, and S. Schacht, J. High Energy Phys. 11 (2017) 061.

[24] R. Aaij *et al.* (LHCb Collaboration), Phys. Rev. Lett. **120,** 121801 (2018).

[25] T. D. Cohen, H. Lamm, and R. F. Lebed, J. High Energy Phys. 09 (2018) 168.

[26] S. Aoki *et al.* (Flavour Lattice Averaging Group), arXiv:1902.08191.

[27] H. Na, C. M. Bouchard, G. P. Lepage, C. Monahan, and J. Shigemitsu (HPQCD Collaboration), Phys. Rev. D **92,** 054510 (2015); **93,** 119906(E) (2016).

[28] J. A. Bailey *et al.* (MILC Collaboration), Phys. Rev. D **92,** 034506 (2015).

[29] E. McLean, C. T. H. Davies, J. Koponen, and A. T. Lytle, arXiv:1906.00701.

[30] W. Detmold, C. Lehner, and S. Meinel, Phys. Rev. D **92,** 034503 (2015).

[31] F. U. Bernlochner, Z. Ligeti, D. J. Robinson, and W. L. Sutcliffe, Phys. Rev. Lett. **121,** 202001 (2018).

[32] A. Berns and H. Lamm, J. High Energy Phys. 12 (2018) 114.

[33] C. W. Murphy and A. Soni, Phys. Rev. D **98,** 094026 (2018).

[34] A. Cerri *et al.*, arXiv:1812.07638.

[35] B. Hamilton and H. Jawahery (private communication).

[36] C. G. Boyd, B. Grinstein, and R. F. Lebed, Phys. Lett. B **353,** 306 (1995).

[37] C. G. Boyd, B. Grinstein, and R. F. Lebed, Phys. Rev. D **56,** 6895 (1997).

[38] B. Grinstein and R. F. Lebed, Phys. Rev. D **92,** 116001 (2015).

[39] B. Colquhoun, C. Davies, J. Koponen, A. Lytle, and C. McNeile (HPQCD Collaboration), Proc. Sci., LATTICE2016 (**2016**) 281 [arXiv:1611.01987]; A. Lytle (private communication).

[40] M. Wirbel, B. Stech, and M. Bauer, Z. Phys. C **29**, 637 (1985).

[41] J. D. Richman and P. R. Burchat, Rev. Mod. Phys. **67**, 893 (1995).

[42] N. Isgur and M. B. Wise, Phys. Lett. B **232**, 113 (1989).

[43] N. Isgur and M. B. Wise, Phys. Lett. B **237**, 527 (1990).

[44] T. Mannel, W. Roberts, and Z. Ryzak, Nucl. Phys. **B355**, 38 (1991).

[45] E. E. Jenkins, M. E. Luke, A. V. Manohar, and M. J. Savage, Nucl. Phys. **B390**, 463 (1993).

[46] V. V. Kiselev, A. K. Likhoded, and A. I. Onishchenko, Nucl. Phys. **B569**, 473 (2000).

[47] A. F. Falk, H. Georgi, B. Grinstein, and M. B. Wise, Nucl. Phys. **B343**, 1 (1990).

[48] V. V. Kiselev, arXiv:hep-ph/0211021.

[49] J. A. Bailey *et al.* (Fermilab Lattice and MILC Collaborations), Phys. Rev. D **89**, 114504 (2014).

[50] J. Harrison, C. Davies, and M. Wingate (HPQCD Collaboration), Phys. Rev. D **97**, 054502 (2018).

[51] E. McLean, C. T. H. Davies, A. T. Lytle, and J. Koponen, Phys. Rev. D **99**, 114512 (2019).

[52] C. G. Boyd, B. Grinstein, and R. F. Lebed, Phys. Rev. Lett. **74**, 4603 (1995).

[53] C. G. Boyd and R. F. Lebed, Nucl. Phys. **B485**, 275 (1997).

[54] C. G. Boyd, B. Grinstein, and R. F. Lebed, Nucl. Phys. **B461**, 493 (1996).

[55] S. C. Generalis, J. Phys. G **16**, 785 (1990).

[56] L. J. Reinders, H. R. Rubinstein, and S. Yazaki, Phys. Lett. **97B**, 257 (1980); **100B**, 519(E) (1981).

[57] L. J. Reinders, S. Yazaki, and H. R. Rubinstein, Phys. Lett. **103B**, 63 (1981).

[58] L. J. Reinders, H. Rubinstein, and S. Yazaki, Phys. Rep. **127**, 1 (1985).

[59] A. Djouadi and P. Gambino, Phys. Rev. D **49**, 3499 (1994); **53**, 4111(E) (1996).

[60] R. Aaij *et al.* (LHCb Collaboration), Phys. Rev. D **95**, 032005 (2017).

[61] A. M. Sirunyan *et al.* (CMS Collaboration), Phys. Rev. Lett. **122**, 132001 (2019).

[62] E. J. Eichten and C. Quigg, Phys. Rev. D **99**, 054025 (2019).

[63] B. Aubert *et al.* (*BABAR* Collaboration), Phys. Rev. Lett. **104**, 011802 (2010).

[64] R. Glattauer *et al.* (Belle Collaboration), Phys. Rev. D **93**, 032006 (2016).

[65] J. P. Lees *et al.* (*BABAR* Collaboration), Phys. Rev. Lett. **123**, 091801 (2019).

[66] See Supplemental Material at http://link.aps.org/supplemental/10.1103/PhysRevD.100.094503 for full set of coefficients and the correlation matrix

[67] A. Le Yaouanc, L. Oliver, and J.-C. Raynal, Phys. Rev. D **79**, 014023 (2009).

[68] R. Aaij *et al.* (LHCb Collaboration), Phys. Rev. D **96**, 112005 (2017).

[69] K. Azizi, Y. Sarac, and H. Sundu, Phys. Rev. D **99**, 113004 (2019).

[70] A. Abdesselam *et al.* (Belle Collaboration), in *10th International Workshop on the CKM Unitarity Triangle (CKM 2018) Heidelberg, Germany, 2018* (2019).

[71] Z.-R. Huang, Y. Li, C.-D. Lu, M. A. Paracha, and C. Wang, Phys. Rev. D **98**, 095018 (2018).

[72] M. Blanke, A. Crivellin, S. de Boer, T. Kitahara, M. Moscati, U. Nierste, and I. Nisandzic, Phys. Rev. D **99**, 075006 (2019).

[73] M. Blanke, A. Crivellin, T. Kitahara, M. Moscati, U. Nierste, and I. Nisandzic, Phys. Rev. D **100**, 035035 (2019).

[74] A. Vaquero, C. DeTar, A. X. El-Khadra, A. S. Kronfeld, J. Laiho, and R. S. Van de Water, in *17th Conference on Flavor Physics and CP Violation (FPCP 2019) Victoria, BC, Canada* (2019).